The role of sulfur in the formation of magmatic-hydrothermal copper-gold deposits

Originally published in:
Earth and Planetary Science Letters 282(1-4), https://doi.org/10.1016/j.epsl.2009.03.036

This is the Green Open Access version of: Seo, J. H., Guillong, M., Heinrich, C. A., 2008. The role of sulfur in the formation of magmatic-hydrothermal copper – gold deposits. *Earth and Planetary Science Letters*, vol. 282, pp. 323-328.
Original publication see: https://doi.org/10.1016/j.epsl.2009.03.036

The role of sulfur in the formation of magmatic-hydrothermal copper – gold deposits

Jung Hun Seo[a*], Marcel Guillong[a], Christoph A. Heinrich[a]

[a]Isotope Geochemistry and Mineral Resources, Department of Earth Sciences, ETH Zurich, 8092 Zurich, Switzerland

*Corresponding author

Jung Hun SEO (seo@erdw.ethz.ch), Marcel GUILLONG (guillong@erdw.ethz.ch), Christoph A. HEINRICH (heinrich@erdw.ethz.ch)

Keywords: Sulfur, Copper, Vapor, Low-density hydrothermal fluids, Porphyry deposit

ABSTRACTS

Essential resources of many rare metals including copper, zinc, molybdenum, silver and gold occur in natural sulfide mineral deposits. Understanding the origin of these metal resources has been limited by a lack of data about the geochemistry of sulfur, the most important and abundant element of ore deposits. We report the first directly measured sulfur concentrations in high-temperature fluids, together with their ore-metal contents, using a new method for sulfur quantification in fluid inclusions by laser ablation inductively coupled plasma mass spectrometry (LA-ICP-MS).
Co-genetic brine and vapor inclusions from magmatic-hydrothermal ore deposits and granitic intrusions show an excess of sulfur over ore metals, as required for efficient ore-mineral precipitation. The results demonstrate that S, Cu and Au are highly enriched in vapor-like magmatic fluids, implying that such low-salinity fluids are the key agent for the formation of porphyry copper and epithermal gold deposits.

1. Introduction

Sulfur is arguably the most important chemical element in the formation of ore deposits, because of the chalcophile geochemical nature of most economically important trace metals in the oxide-dominated lithosphere of our planet. Sulfur is a major component in volcanic fluids (Hedenquist et al., 1993) and magmatic-hydrothermal ores including porphyry-copper, skarn and polymetallic vein deposits, where it is enriched to a greater degree than any of the ore metals themselves. Individual porphyry-copper deposits are crustal sulfur anomalies commonly exceeding 1 billion tons of sulfur (Gustafson and Hunt, 1975). In such ore deposits, sulfur is required for the precipitation of the economically important sulfide minerals such as chalcopyrite ($CuFeS_2$) and molybdenite (MoS_2) and is present in even greater quantities as pyrite (FeS_2) and anhydrite ($CaSO_4$). These minerals reflect sulfur

transport in hydrothermal fluids as reduced (sulfide) as well as oxidized species (sulfur dioxide and sulfate) (Webster and Mandeville, 2007). Sulfide is also an essential ligand in metal-transporting fluids, enhancing the solubility of gold and possibly copper by formation of stable metal-sulfide complexes (Mountain and Seward, 2003; Stefánsson and Seward, 2004) in subcritical aqueous solutions, as required for the formation of bonanza-grade epithermal gold deposits (e.g., Fig. 1) (Ronacher et al., 2004). At temperatures above ~ 350°C and in fluids of lower than liquid-like density (<< 1g cm^{-3}), the relative importance of sulfur and chloride complexes for hydrothermal transport of different ore metals has not yet been well established experimentally (Seward and Barnes, 1997).

Differences in the thermodynamic stability of chloride and sulfide species are particularly important for selective metal transport in saline two-phase hydrothermal systems existing above the critical point of pure water, where hypersaline liquid (brine) coexists and may physically separate from a lower-salinity vapor phase. Microanalysis of natural inclusions of coexisting brine and vapor show that the brine preferentially carries all major salts including NaCl, KCl, $FeCl_2$, as well as minor and trace metals such as Mn, Zn, Rb, Cs and Pb. Some of the vapor phase is selectively enriched in Cu and Au (Audétat et al., 1998; Heinrich et al., 1999), but the chemical reason for selective metal fractionation into the vapor is debated (Mavrogenes et al., 2002; Cauzid et al., 2007). Recent experiments (Simon et al., 2006; Nagaseki and Hayashi, 2008; Pokrovski et al., 2008) support the interpretation that the formation of relatively volatile Cu and Au complexes with sulfur in some conditions is responsible for the partitioning into low-density magmatic vapor.

Here, we report concentrations of sulfur, copper, gold, arsenic, molybdenum, cesium, lead and the major salt components sodium, potassium and iron in natural co-genetic vapor and brine inclusions trapped along individual healed microcracks in quartz (so-called "boiling assemblages"; Heinrich et al., 1999) to understand the role of sulfur in high-temperature metal segregation by fluid phase separation.

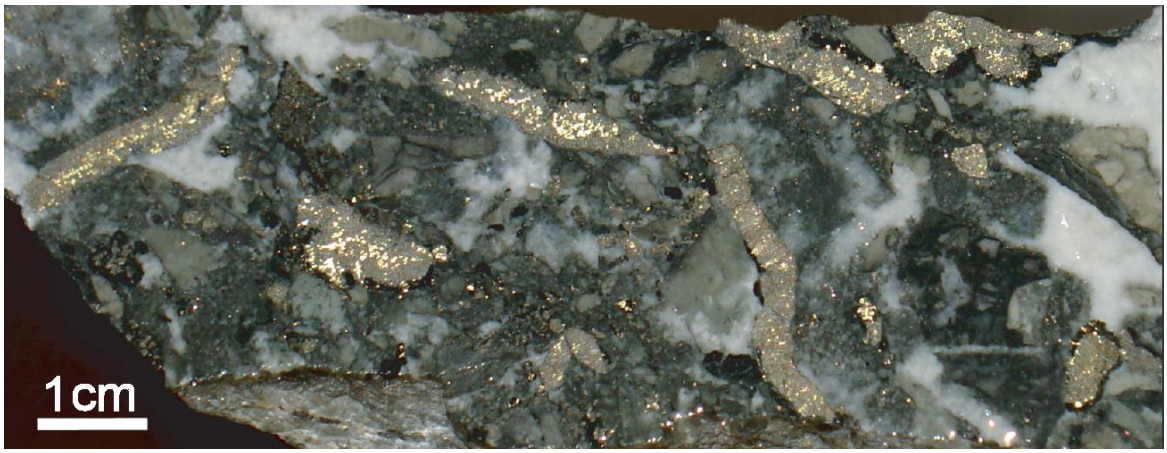

Figure 1. Bonanza-grade ore from the giant epithermal gold deposit of Porgera (Papua New Guinea). Several weight % of gold (bright yellow spots) in this hydrothermal breccia were co-precipitated with pyrite (dull brown aggregates) from a low-salinity aqueous fluid that suddenly started to boil upon ascent from an underlying igneous intrusion (Ronacher et al., 2004). Inclusion microanalyses from deeper-seated magmatic-hydrothermal environments reported in this paper imply that such extreme precious metal enrichments (107 fold compared to average crustal gold abundance) are effected by extremely gold and sulfur-rich fluids derived from high-temperature magmatic vapor.

2. Samples descriptions and inclusion microthermometry

Selected quartz crystals from two porphyry style Cu-Au-Mo deposits (Bingham Canyon, USA and Bajo de la Alumbrera, Argentina), two granite related Sn-W veins [Zinnwald, Germany; Heinrich et al. (1999) and Mole Granite, Australia; Audétat et al. (2000)], and barren miarolitic cavities from a granitoid intrusion without associated ore deposits [Rito del Medio Pluton, USA; Audétat and Pettke (2003)] contain assemblages of vapor and brine that coexisted at high temperatures (320-490℃) and pressures (90-480 bar) (table 1). Based on petrography and consistent microthermometric properties, the fluid inclusions have not suffered modification after entrapment, except for likely diffusional exchange of hydrogen (Mavrogenes and Bodnar, 1994). Salinities of individual inclusions were measured by microthermometry, before *in-situ* analysis by LA-ICP-MS. Apparent salinity from microthermometry was combined with element ratios measured by LA-ICP-MS to obtain absolute element concentrations, using Na as an internal standard and an empirical correction for the effects of the other salts (Günther et al., 1998; Heinrich et al, 2003). As a result of this calibration, absolute element concentrations are subject to potential systematic errors, whereas the directly measured element ratios are reliable within the precision of LA-ICP-MS analysis. Homogenization temperatures of the brine inclusions in the assemblages range from 323 ± 8 to 492 ± 8 °C and can be combined with the brine salinities (wt% NaCl eq.) to estimate the P-T conditions of brine + vapor entrapment, using the limiting two-phase surface of the NaCl-H_2O model system (Driesner and Heinrich, 2007) (Table 1).

Table 1. Salinities (equivalent NaCl wt %), homogenization temperatures (T_h), Bulk S molality, and Cl molalities (calculated from salinities) of 11 co-genetic brine and vapor inclusions, with estimated pressures of entrapment and densities of the fluids calculated by using the limiting two-phase surface NaCl-H_2O model system (Driesner and Heinrich, 2007). "ND" represent not determined values.

Location	Type	Sample name	T_h (°C)	Pressure (bar)	Density (g/cm^3)	Salinity (eqv. NaCl wt%)	Total S (mol/kg)	Total Cl (mol/kg)
Bingham Canyon	Brine	A35-4561	323 ± 8	88	1.04	34.7 ± 1.8	0.240	5.9
Quartz stockwork vein	Vapor				0.70	6.2 ± 1.1	0.149	1.1
Bingham Canyon	Brine	JH2_a7	429 ± 8	221	1.10	50.4 ± 0.4	0.550	8.6
Molybdenite-quartz vein	Vapor				0.50	7.9 ± 3.2	0.390	1.3
Bingham Canyon	Brine	JH2_BT2	492 ± 8	434	0.90	41.7 ± 2.1	0.190	7.1
Molybdenite-quartz vein	Vapor				0.50	7.4 ± 3.1	0.167	1.3
Rito del Medio	Brine	Rito8_D	480 ± 8	477	0.84	26.3 ± 0.0	0.178	4.5
Quartz, miarolitic cavity	Vapor				0.40	4.2 ± 3.3	0.063	0.7
Rito del Medio	Brine	Rito8_C	435 ± 8	311	0.90	29.7 ± 0.1	0.189	5.1
Quartz, miarolitic cavity	Vapor				0.30	2.1 ± 0.7	0.085	0.4
Zinnwald	Brine	Zin1_TP1	453 ± 8	364	0.80	30.4 ± 0.7	0.068	5.2
Quartz - cassiterite vein	Vapor				0.40	3.7 ± 0.1	0.300	0.6
Mole Granite, Gold	Brine	gold_1.2.2	356 ± 19	126	1.03	37.4 ± 0.4	0.012	6.4
Bismuth-rich quartz vein	Vapor				0.59	2.4 ± 0.5	0.155	0.4
Mole Granite, Trewhellas	Brine	BoydB_1	329 ± 3	88	1.09	39.6 ± 0.4	0.028	6.8
Quartz-topaz greisen	Vapor				0.68	3.3 ± -	0.201	0.6
Mole Granite, Balmains	Brine	Loww_9D	431 ± 3	282	0.92	35.1 ± 0.2	0.007	6.0
Quartz vein in W deposit	Vapor				0.48	2.0 ± 0.0	0.110	0.3
Mole Granite, Balmains	Brine	Loww_9.1	440 ± 3	262	1.04	46.1 ± 0.7	0.007	7.9
Quartz vein in W deposit	vapor				0.48	2.1 ± -	0.030	0.4
Bajo de la Alumbrera	Brine	80-1	ND	ND	ND	34.7 ± 2.0	0.183	5.9
Quartz (-pyrite)- vein	Vapor				ND	7.5 ± 1.6	0.100	1.3

3. Analytical methods

Our technique for simultaneous quantification of sulfur and selected elements in vapor and brine inclusions uses a beam-homogenized 193 nm excimer laser ablation system (Geolas, ETH prototype) connected to an ICP-MS (Perkin Elmer Elan 6100 DRC) which was tuned for sulfur detection. To establish and validate the quantification of sulfur in fluid inclusions, we first measured 30 individual brine inclusions from a presumably homogeneous assemblage formed in a single healed crack having similar salinities (42.4 ± 1.2 NaCl equiv. wt%), using two different ICP-MS instruments: a sector-field MS (Thermo – Finnigan ELEMENT-2) and the quadrupole MS. The sector-field instrument allows sufficiently high mass resolution to resolve polyatomic interferences ($^{16}O^{16}O^{+}$) on sulfur ($^{32}S^{+}$). The comparison showed that precision and accuracy of sulfur quantification is not primarily limited by mass interferences, but by a so far unknown contamination that is released from the ablation cell during quartz ablation (Guillong et al., 2008). The key to successful quantification of sulfur concentrations in fluid inclusions is therefore a very careful baseline correction, which leads to accurate results despite a relatively large uncertainty of 35% RSD among the 30 co-genetic inclusions. Limits of detection for sulfur in fluid inclusions depend on inclusion size and reach down to 100 µg/g for large (60 µm) inclusions (Guillong et al., 2008).

We used a reduced set of isotopes, i.e. ^{23}Na, ^{29}Si, ^{39}K, ^{57}Fe, ^{65}Cu, ^{75}As, ^{95}Mo, ^{133}Cs, ^{197}Au, ^{208}Pb and ^{32}S, with increased dwell times of 50 ms for ^{197}Au and 20 ms for ^{32}S compared to 10 ms for all other elements, to reduce the limit of detection especially for gold. Addition of small amounts of H_2 gas to the He carrier gas increases the sensitivity of selective elements (notably for Cu, Au, Mo) and thus improves their limit of detection (Guillong and Heinrich, 2007). Chlorine is calculated from microthermometric apparent salinity and charge-balance, incorporationg the cation ratios for each inclusion analysed by LA-ICP-MS.

4. Results

Results from 11 assemblages of coexisting magmatic-hydrothermal brine and vapor inclusions show that NaCl, KCl, $FeCl_2$, Cu and S are the dominant components, constituting > 97% of the entire solute content in both fluid types (Table 2 and 3). Sulfur concentrations are similar to the concentrations of copper, or even exceed those of copper (Fig. 2) and all other chalcophile metals (Mo, Pb) in both fluid phases. A positive correlation between sulfur and copper is accentuated if concentrations are normalized to Na, the generally dominant cation component (Fig. 2c). Many of the absolute S and Cu concentrations and the more reliable S/Na and Cu/Na ratios follow a correlation line with slope 1 on the mass scale (Fig. 2), which corresponds to a molar ratio of S : Cu ~ 2 : 1 considering the atomic weights of copper (63.55 g/mol) and sulfur (32.06 g/mol). Relative to Na and other salt components, both S and Cu are enriched in the vapor compared to coexisting brine inclusions (Fig. 2c), but in some assemblages the absolute concentrations of copper and sulfur are higher in the brine inclusions than in the vapor inclusions (e.g. Rito del Medio Pluton, Bingham Canyon and Bajo de la Alumbrera; Figs. 2a and 2b). Results for the vapor/liquid partitioning of all analyzed elements are summarized in Figure 3, normalized to Pb which fractionates most strongly into saline brines due to stable chloride complexation with high ligand numbers (≥ 2) (Seward, 1984). Pb, Fe, Cs, K and Na show similar fractionation behavior with strong preference for the brine. Mo, As, Au, Cu and S exhibit increasing relative preference for the vapor phase, whereby the degrees of partitioning for Au, Cu and S into the vapor phase are clearly correlated. There are two groups of assemblages, marked by boxes in Figure 3, whose partitioning behavior also correlates with the geological environment of the respective samples. In all samples from Sn-W deposits, the ratios Cu/Pb and S/Pb as well as

Table 2. Fluid inclusion analyses, showing averages (µg/g) and standard deviations (1 sigma; SD) of 3-15 individual brine and vapor inclusions trapped at the same time on a single microfracture. LA-ICP-MS analyses of element ratios were first calibrated against NIST 610 as external standard, and then recast into approximate absolute concentrations based on apparent total salinity based on previous microthermometry. It was assumed that wt% NaCl equivalent from microthermometry is equal to wt% NaCl + 0.5• wt% $FeCl_2$ + 0.5• wt% KCl (Günther et al., 1998; Heinrich et al., 2003), ignoring the fact that Cu and S are major components especially in the vapor inclusions which introduces a potential systematic error in all absolute concentrations. Therefore, element ratios as plotted in Figures 2c and 3 are analytically more reliable than the concentrations shown in Figures 2a and 2b.

Location	Type		µg/g	^{23}Na	^{32}S	^{39}K	^{57}Fe	^{65}Cu	^{75}As	^{95}Mo	^{133}Cs	^{197}Au	^{208}Pb
Bingham Canyon	Brine	A35-4561	Average	97 000	7 600	52 000	37 000	7 600	57.0	450.0	64.0	0.14	2 800
Quartz stockwork vein			SD	17 300	4 600	43 000	11 200	6 100	38.0	440.0	47.0	0.06	1 770
	Vapor		Average	16 800	4 800	8 400	7 500	4 200	50.0	51.0	15.0	0.64	390
			SD	3 610	3 000	4 100	2 900	2 600	58.0	45.0	14.0	0.64	240
Bingham Canyon	Brine	JH2_a7	Average	129 000	17 600	117 000	55 000	18 900	14.3	33.0	43.0	0.31	3 000
Molybdenite-quartz vein			SD	3 800	2 300	8 700	4 900	7 500	3.8	32.0	4.0	0.12	230
	Vapor		Average	23 000	12 400	13 400	7 200	10 800	25.0	18.3	6.8	1.40	440
			SD	8 400	10 300	5 600	5 100	10 300	12.6	18.2	4.4	ND	250
Bingham Canyon	Brine	JH2_BT2	Average	117 000	6 000	79 000	39 000	1 190	51.0	88.0	42.0	1.28	3 800
Molybdenite-quartz vein			SD	10 500	3 200	10 700	13 000	950	31.0	87.0	7.0	1.03	970
	Vapor		Average	22 000	5 400	11 200	7 000	300	148.0	21.0	9.3	3.70	540
			SD	3 800	2 500	3 400	1 790	240	29.0	ND	6.9	2.90	470
Rito del Medio	Brine	Rito8_D	Average	81 000	5 700	37 000	18 300	1 230	270.0	128.0	1 020.0	0.38	2 300
Quartz, miarolitic cavity			SD	3 700	700	6 100	7 400	410	44.0	20.0	230.0	0.29	480
	Vapor		Average	13 300	2 000	5 300	3 200	290	196.0	13.9	178.0	0.45	370
			SD	1 018	690	1 970	1 100	210	91.0	9.8	139.0	0.45	82
Rito del Medio	Brine	Rito8_C	Average	95 000	6 100	34 000	18 600	1 340	177.0	82.0	720.0	0.14	2 400
Quartz, miarolitic cavity			SD	4 600	1 730	13 500	4 600	400	37.0	23.0	340.0	0.08	440
	Vapor		Average	7 000	2 700	3 200	1 510	430	93.0	47.0	45.0	0.45	120
			SD	790	1 520	1 590	1 220	330	51.0	46.0	17.3	0.45	55
Zinnwald	Brine	Zin1_TP1	Average	93 000	2 200	48 000	19 200	32	1030.0	4.4	3 300.0	0.34	53 000
Quartz - cassiterite vein			SD	3 100	940	6 700	4 000	28	157.0	3.6	900.0	0.07	10900
	Vapor		Average	12 000	9 700	4 600	2 500	2 600	690.0	14.8	221.0	2.50	3900
			SD	1 920	3 100	4 400	2 000	1 400	360.0	ND	88.0	1.91	1850
Mole Granite, Gold	Brine	gold_1.2.2	Average	75 000	390	66 000	107 000	250	187.0	1.1	3 000.0	0.03	8 700

Bismuth-rich quartz vein			SD	9 700	105	10 200	14 400	110	151.0	0.6	420.0	0.02	1 900
	Vapor		Average	7 300	5 000	2 400	4 200	4 300	280.0	1.2	93.0	0.42	320
			SD	1 200	1 640	700	980	3 000	200.0	ND	38.0	0.25	60
Mole Granite, Trewhellas	Brine	BoydB_1	Average	81 000	900	73 000	106 000	190	87.0	6.9	3 300.0	0.34	3 600
Quartz-topaz greisen			SD	7 000	340	7 300	10 300	52	49.0	6.8	370.0	0.34	790
	Vapor		Average	9 900	6 500	2 800	4 500	3 700	60.0	12.9	133.0	0.51	170
			SD	880	2 300	810	1 220	900	22.0	1.9	25.0	0.18	32
Mole Granite, Trewhellas	Brine	Loww_9D	Average	83 000	220	56 000	76 000	161	80.0	1.5	2 500.0	0.06	4 200
Quartz-topaz greisen			SD	5 100	130	6 200	6 800	55	43.0	0.8	390.0	0.04	480
	Vapor		Average	6 400	3 500	2 800	1 390	540	200.0	4.7	123.0	0.37	80
			SD	590	2 500	1 280	1 120	230	92.0	5.6	52.0	0.27	38
Mole Granite, Trewhellas	Brine	Loww_9.1	Average	109 000	230	73 000	101 000	180	86.0	1.3	3 200.0	0.19	5 200
Quartz-topaz greisen			SD	17 500	140	18 200	24 000	68	46.0	0.5	880.0	0.18	970
	vapor		Average	5 200	960	2 800	4 900	360	8.8	1.2	132.0	0.05	260
			SD	390	820	400	720	310	1.5	1.5	23.0	0.01	60
Bajo de la Alumbrera	Brine	80-1	Average	78 000	5 900	50 000	84 000	6 500	ND	ND	19.1	0.38	1 420
Quartz (-pyrite)- vein			SD	8900	20	14 500	22 000	2 500	ND	ND	11.5	0.26	440
	Vapor		Average	24 000	3 200	7 400	8 800	1 800	ND	ND	7.2	0.77	210
			SD	9200	760	1 100	1 270	2 300	ND	ND	1.8	0.56	151

Table 3. Inclusion analyses recast into molalities (mol/kg H_2O) of nominal solute components NaCl, KCl, $FeCl_2$, $As(OH)_3$, $Mo(OH)_2$, CsCl, $PbCl_2$, Au, CuS_2 and H_2S. Recalculation is based on the analyzed element concentrations of Na, K, Fe, As, Mo, Cs, Pb, Au, Cu and S of Table 2; Cl is not measured and assumed from stoichiometry and total apparent salinity given in Table 1 (Heinrich et al., 2003). The nominal component CuS_2 reflects possible species like $Cu(HS)(H_2S)^0$, $Cu(HS)_2^-$ or $Cu(HS)(SO_2)^0$ in solution and also corresponds to the stoichiometric ratio of Cu:S = 1:2 in chalcopyrite ($CuFeS_2$), the dominant and first-saturating sulfide phase in most porphyry-copper deposits. The last two columns of the table list the total sulfur, and the total sulfur minus two times the molality of Fe. This difference measures the sulfur vs. iron mass-balance upon precipitation of chalcopyrite ($CuFeS_2$) and pyrite (FeS_2), which constitutes an important 'chemical divide' in the chemical evolution of hydrothermal fluids upon cooling, as discussed in the manuscript.

Location	Type		Recalculated analysis in mol/kg water of nominal solute components									Total S (mol/kg)	S – 2Fe (mol/kg)
			NaCl	KCl	$FeCl_2$	$As(OH)_3$	$Mo(OH)_2$	CsCl	$PbCl_2$	Au	CuS_2	H_2S		
Bingham Canyon	Brine	A35-4561	4.20	1.34	0.66	0.001	0.0046	0.000	0.014	7.1E-07	0.120	-0.002	0.240	-1.080
Quartz stockwork vein	Vapor		0.73	0.22	0.14	0.001	0.0005	0.000	0.002	3.2E-06	0.067	0.016	0.149	-0.121

Bingham Canyon	Brine	JH2_a7	5.60	3.00	0.98	0.000	0.0003	0.000	0.014	1.6E-06	0.300	-0.045	0.550	-1.420
Molybdenite-quartz vein	Vapor		1.00	0.34	0.13	0.000	0.0002	0.000	0.002	7.1E-06	0.171	0.047	0.390	0.129
Bingham Canyon	Brine	JH2_BT2	5.10	2.00	0.70	0.001	0.0009	0.000	0.018	6.5E-06	0.019	0.150	0.188	-1.200
Molybdenite-quartz vein	Vapor		0.95	0.29	0.13	0.002	0.0002	0.000	0.003	1.9E-05	0.005	0.157	0.167	-0.084
Rito del Medio	Brine	Rito8_D	3.50	0.95	0.33	0.004	0.0013	0.008	0.011	1.9E-06	0.019	0.139	0.178	-0.480
Quartz, miarolitic cavity	Vapor		0.58	0.14	0.06	0.003	0.0001	0.001	0.002	2.3E-06	0.005	0.054	0.063	-0.051
Rito del Medio	Brine	Rito8_C	4.20	0.88	0.33	0.002	0.0008	0.005	0.012	6.9E-07	0.021	0.147	0.189	-0.480
Quartz, miarolitic cavity	Vapor		0.30	0.08	0.03	0.001	0.0005	0.000	0.001	2.3E-06	0.007	0.072	0.085	0.031
Zinnwald	Brine	Zin1_TP1	4.00	1.23	0.34	0.014	0.0000	0.025	0.250	1.7E-06	0.001	0.067	0.068	-0.620
Quartz - cassiterite vein	Vapor		0.52	0.12	0.04	0.009	0.0002	0.002	0.019	1.2E-05	0.032	0.240	0.300	0.212
Mole Granite, Gold	Brine	gold_1.2.2	3.20	1.69	1.92	0.002	0.0000	0.023	0.042	1.5E-07	0.004	0.004	0.012	-3.800
Bismuth-rich quartz vein	Vapor		0.32	0.06	0.08	0.004	0.0000	0.001	0.002	2.1E-06	0.068	0.020	0.155	0.005
Mole Granite, Trewhellas	Brine	BoydB_1	3.50	1.87	1.90	0.001	0.0001	0.025	0.017	1.7E-06	0.003	0.022	0.028	-3.800
Quartz-topaz greisen	Vapor		0.43	0.07	0.08	0.001	0.0001	0.001	0.001	2.6E-06	0.059	0.083	0.200	0.040
Mole Granite, Balmains	Brine	Loww_9D	3.60	1.43	1.36	0.001	0.0000	0.019	0.020	3.1E-07	0.003	0.002	0.007	-2.700
Quartz vein in W deposit	Vapor		0.28	0.07	0.02	0.003	0.0000	0.001	0.000	1.9E-06	0.009	0.093	0.110	0.060
Mole Granite, Balmains	Brine	Loww_9.1	4.70	1.87	1.81	0.001	0.0000	0.024	0.025	9.4E-07	0.003	0.001	0.007	-3.600
Quartz vein in W deposit	vapor		0.23	0.07	0.09	0.000	0.0000	0.001	0.001	2.6E-07	0.006	0.019	0.030	-0.146
Bajo de la Alumbrera	Brine	80-1	3.40	1.28	1.51	ND	ND	0.000	0.007	1.9E-06	0.103	-0.023	0.183	-2.800
Quartz (-pyrite) - vein	Vapor		1.03	0.19	0.16	ND	ND	0.000	0.001	3.9E-06	0.028	0.044	0.100	-0.210

the absolute concentrations of Cu and S are significantly higher in the vapors than in the brines. In porphyry-Cu-Mo-Au deposits and the Rito del Medio pluton (barren intermediate-composition intrusion), Cu and S are enriched in the vapor relative to other salt components like Pb and Na, but their absolute concentrations in the vapor are commonly smaller than in the brine. However, both fluid phases in porphyry-Cu-Mo-Au are higher in total S, Cu and Au compared with the absolute concentration of these elements in the Sn-W mineralizing fluids.

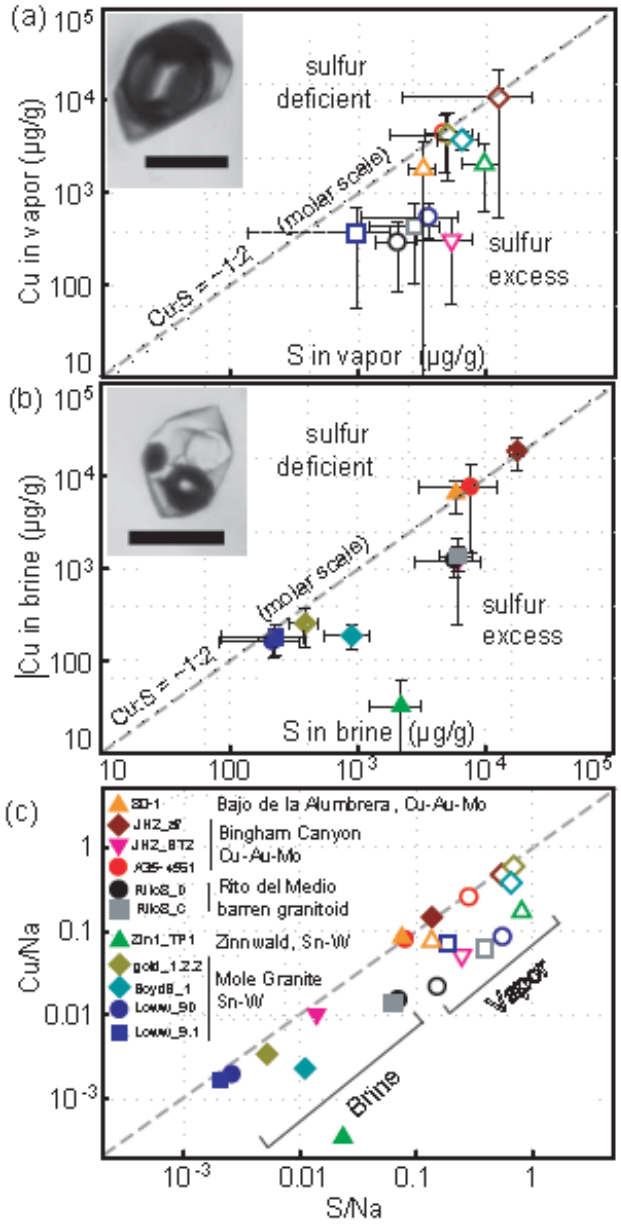

Figure 2. Concentrations of sulfur and copper in natural magmatic-hydrothermal fluid inclusions. Co-genetic pairs of vapor + brine inclusions ("boiling assemblages") in high-temperature hydrothermal veins from porphyry Cu-Au-Mo deposits (orange to red symbols), granite related Sn-W deposits (blue - green), and a barren granitoid (black - gray) are shown. All vapor (a) and brine inclusions (b) have sulfur concentrations equal to copper or contain an excess of sulfur (the S : Cu = 1 : 1 line approximates a 2 : 1 molar ratio). Element ratios (c), which are not influenced by uncertainties introduced by analytical calibration (Heinrich et al., 2003), show an even tighter correlation along and to the right of the molar 2:1 line, with Cu/Na as well as S/Na systematically higher in the vapor inclusions (open symbols) than in the brine inclusions (full symbols). Averages of 3-14 single fluid inclusions in each assemblage from single healed fractures are plotted, with error bars of one standard deviation. Scale bars in the inclusion micrographs represent 50 µm.

5. Discussion

The new results of high sulfur concentrations, which are similar to or even higher than those of Cu, constrain the possible speciation of major components in coexisting magmatic-hydrothermal ore fluids. Even though a full speciation calculation is presently impossible for lack of thermodynamic data, the relative importance of sulfur and chloride as complexing agents for the four main cations in both fluid phases, Na, K, Fe and Cu, can be discussed by considering the following exchange equilibria:

$$CuCl^0 + H_2S \leftrightarrows CuHS^0 + HCl \quad (1a)$$
$$CuCl^0 + 2H_2S \leftrightarrows CuHS\,H_2S^0 + HCl \quad (1b)$$
$$CuCl_2^- + 2H_2S + H^+ \leftrightarrows CuHS\,H_2S^0 + 2\,HCl \quad (1c)$$
$$NaCl^0 + H_2S \leftrightarrows NaHS^0 + HCl \quad (2)$$
$$KCl^0 + H_2S \leftrightarrows KHS^0 + HCl \quad (3)$$
$$FeCl_2^0 + 2H_2S \leftrightarrows Fe(HS)_2^0 + 2HCl \quad (4)$$

Neutral species will be dissociated to variable degrees depending on concentrations, pressure, temperature and acidity (pH) of the system. The high chloride concentration of the dense brine will increasingly favor chloride species like $NaCl^0$, $CuCl^0$ and $FeCl_2^0$ in the liquid phase at high temperatures (Seward and Barnes, 1997; Simon et al., 2004). The low water density and weak dielectric properties of the vapor will preferentially stabilize neutral species, and overall suppress the solubility of all components whose stability depends on hydration of metals and their close-neighbor ligands (Palmer et al., 2004; Williams-Jones et al., 2002). The partitioning of the four major cations between the coexisting fluid phases is therefore governed by their relative tendency to form inner-sphere complexes with the two competing ligand components, Cl and S. In subcritical aqueous solution, copper (I) forms sulfide complexes such as $CuHS^0$ and $Cu(HS)_2^-$ that are more stable than potential sulfide complexes of hard-sphere cations like Na^+, K^+ and Fe^{2+} whose existence is not even confirmed experimentally (Mountain and Seward, 2003). Sulfur is partly present as SO_2 in moderately oxidized magmatic-hydrothermal systems (Giggenbach, 1992), potentially giving rise to mixed sulfide - sulfite complexes with metals (Pokrovski et al., 2008). Pokrovski et al. (2008) recently demonstrated experimentally the preferential stabilization of Cu in the vapor by addition of S. This implies a relative tendency for equilibria like (1) to shift towards Cu-S complexes in the vapor, compared to equilibria like (2) – (4) stabilizing K, Na and Fe as chloride complexes in the brine. However, the experiments (Pokrovski et al., 2008) used much lower Fe concentrations than present in the natural fluids, and the fractionation of Cu to the vapor was not as high as observed in some natural brine + vapor pairs (Heinrich et al., 1999; Fig. 3). The extreme Cu-partitioning to the vapor in some of the natural fluids might be explained by the competition of cations for the limited ligand components, if the concentrations of free $HCl^0 + Cl^-$ and $H_2S^0 + HS^-$ are small compared to the proportion of sulfide and chloride bound in metal complexes, notably $FeCl_2^0$. The large number of fluid inclusion compositions with a molar ratio of S/Cu ~ 2 (Fig. 2) imply that particularly stable copper species with two sulfur ligands (such as neutral HS–Cu–SH_2^0, or possibly HS–Cu–SO_2^0 for vapor, and charged HS–Cu–SH^- for brine analogous to the suggestion of Pokrovski et al. (2008) for Au), may be the predominant species for S as well as Cu in the vapor. Sulfur complexes might even dominate copper speciation in the Na-K-Fe-chloride-rich brines, because these commonly also lie on the S/Cu ~ 2 correlation line, or contain an excess of sulfur (probably in the form of sulfate and/or sulfur dioxide; Fig. 2).

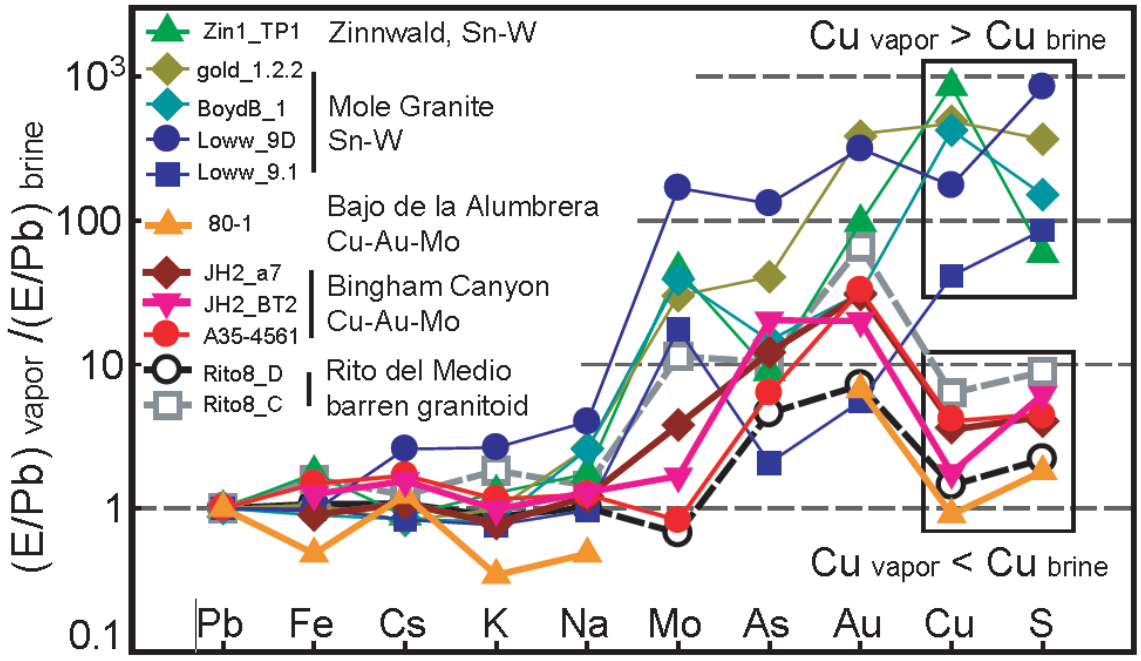

Figure 3. Partitioning of elements between co-genetic vapor and brine inclusions. Fluid analyses including sulfur and gold are normalized to Pb, which is most strongly enriched in the saline brine (Seward, 1984). S, Cu, Au, As and sometimes Mo preferentially fractionate into the vapor relative to the main chloride salts of Pb, Fe, Cs, K and Na. A close correlation between the degrees of vapor fractionation of S, Cu and generally also Au indicates preferential sulfur complexation of these metals in the vapor. The two boxes distinguish assemblages in which absolute concentrations of Cu and S are higher or lower in vapor compared with brine. This grouping correlates with geological environment, i.e., the redox state and pH of the source magmas and the exsolving fluids.

6. Geological implications

The geological significance of our new data for magmatic-hydrothermal ore formation is profound, irrespective of the still tentative interpretations of species stoichiometry. Although the fluid inclusions in this study are trapped at high temperature (320-490 ℃), some of them record the initial stage of ore precipitation and thus may not reflect the unmodified fluids exsolved from the source magma.

Nevertheless, our results indicate that the formation of Cu±Au-rich ore fluids by exsolution from a hydrous magma is not primarily controlled by the salinity of this fluid, as previously thought (Candela and Holland, 1984; Cline and Bodnar, 1991). More likely, the efficiency of copper extraction from the magma is determined by the sulfur concentration in the exsolving fluids. This may in turn be controlled by the presence and amount of a separate sulfide melt phase that decomposes at the time of fluid saturation in the magma (Hattori, 1993), consistent with observations of magmatic sulfide melt inclusions having a Au/Cu ratio that matches the bulk composition of the associated porphyry-Cu-Au deposit (Bajo de la Alumbrera; Halter et al., 2002; Ulrich et al., 1999). The predominance of Cu-S species in primary magmatic fluids is also indicated by very high initial copper concentrations in single-phase ore fluids at Butte (with Cu > Na; Rusk et al., 2004), and by the extreme copper partitioning into some volcanic vapors (Lowenstern et al., 1991). The copper content of these low-salinity fluids greatly exceeds the Cu concentration that would be expected from melt/chloride partitioning experiments (Candela and Holland, 1984).

Partitioning of Cu and S between brine and vapor also appear to be related to differences in source magma compositions, as indicated by two groups of data in Figure 3. In fluid pairs from Sn-W veins, sulfur and copper are most strongly enriched in the vapor inclusions. The source magmas of these fluids typically are reduced (fO_2 < FMQ) and commonly

peraluminous granites, which generate relatively reduced and acid fluids (Lehmann, 1990). Upon cooling and phase separation, H_2S is stabilized in such fluids relative to HSO_4^-. The low pH favors volatile neutral complexes like $HS–Cu–SH_2^0$ as reaction (1c), relative to charged species such as $HS–Cu–SH^-$ that will be less stable in the lower-density vapor (Pokrovski et al., 2008). On the other hand, the fluids in porphyry deposits and the barren granitoid show a weaker tendency for Cu, Au and S to fractionate into the vapor (Fig. 3). These fluids originate from relatively oxidized (fO_2 = NNO or higher) and peralkaline magmas (Beane and Titley, 1981), which will produce oxidized and less acidic fluids. This chemical environment stabilizes charged sulfide species (e.g., $Cu(HS)_2^-$) which are less volatile that their neutral analogues in the saline liquid (Fig. 3). The partitioning trends of copper in the boiling fluids in porphyry environments are consistent with previous sulfur-bearing hydrothermal experiments (Simon et al., 2006). Note however, that the absolute amounts of copper and total sulfur in the fluids from porphyry copper systems is higher, probably because there is overall more sulfur available in subduction-related mafic to intermediate magmas (Hattori, 1993) compared with crustal Sn-W granite magmas.

Upon cooling, brine and vapor can efficiently precipitate their Cu as chalcopyrite ($CuFeS_2$) or bornite (Cu_5FeS_4), the dominant ore minerals in porphyry-copper deposits, because both fluid phases contain a two-fold molar excess of sulfur compared to copper (Fig. 2). The vapor phase will generally make the greater contribution to copper ore deposition, given that it is particularly enriched in Cu and S (Fig. 2, 3) and usually dominates over the brine in terms of mass (Henley and McNabb, 1978; Williams-Jones and Heinrich, 2005; Klemm et al., 2007). Upon further cooling, pyrite (FeS_2) usually precipitates after $CuFeS_2$. The sulfur in each fluid phase remaining after precipitation of most of the Cu and Fe as Cu-Fe-sulfides and pyrite is available as complexing ligand or for the deposition of other sulfide minerals at lower temperature. This sulfur quantity is determined by the difference between the initial molalities of sulfur ($m_{s,tot}$) minus the iron (m_{Fe}) required to make $CuFeS_2$ and FeS_2. In our analyses, this difference, $m_{S,tot} - 2 \bullet m_{Fe}$, is systematically negative for the brines, but variably positive for some vapors (Table 3). All brines have an iron excess relative to sulfur, whereas many vapors have a sulfur excess over the Fe (and Cu) required to precipitate $CuFeS_2$ and FeS_2. Brines with iron excess will become exhausted in sulfide upon cooling, are therefore unable to transport S-complexed trace metals like Au to lower temperatures. Such brines would require an external source of sulfide for effective precipitation of base metals like PbS and ZnS at lower temperatures (Heinrich, 2006), for example in post-magmatic ore deposits hosted by sedimentary basins (Stoffell et al., 2008). By contrast, the vapors containing an excess of sulfur will be able to transport sulfide-complexed metals —notably gold— to lower temperatures when the magmatic vapor cools and contracts to an aqueous liquid (Heinrich et al., 2004). Such a process is favorable, and sulfur excess is probably essential, for the extreme precious-metal enrichment forming giant epithermal gold deposits such as Porgera (Fig. 1).

More generally, our new analyses demonstrate that the sulfur balance during fluid phase separation constitutes a first-order chemical divide for the formation of different types of hydrothermal ore deposits in the earth's crust.

Acknowledgements

We thank A. Audétat for selected samples and D. Meier for Alumbrera data. Discussion with T. Driesner, H. Murakami and C. Sanchez-Valle, and helpful comments by G. S. Pokrovski and an anonymous reviewer are greatfully acknowledged. Funded by Swiss NSF Grant 200020-116693/1.

References

Audétat, A., Günther, D., Heinrich, C. A., 1998. Formation of a magmatic-hydrothermal ore deposit: Insights with LA-ICP-MS analysis of fluid inclusions. Science 279, 2091-2094.

Audétat, A., Günther, D., Heinrich, C. A., 2000. Causes for large-scale metal zonation around mineralized plutons: fluid inclusion LA-ICP-MS evidence from the Mole Granite, Australia. Econ. Geol. 95, 1563-1581.

Audétat, A., Pettke, T., 2003. The magmatic-hydrothermal evolution of two barren granites: A melt and fluid inclusion study of the Rito del Medio and Cañada Pinabete plutons in northern New Mexico (USA). Geochim. Cosmochim. Acta 67, 97-121.

Beane, R. E., Titley, S. R., 1981. Porphyry copper deposit; Part II. Hydrothermal alteration and mineralization, Econ. Geol. 75th Anniv. vol., 235-269.

Candela P. A., Holland H. D., 1984. The partitioning of copper and molybdenum between silicate melts and aqueous fluids. Geochim. Cosmochim. Acta 48, 373–380.

Cauzid, J., Philippot, P., Martinez-Criado, G., Ménez, B., Labouré, S., 2007. Contrasting Cu-complexing behaviour in vapor and liquid fluid inclusions from the Yankee Lode deposit, Mole Granite, Australia. Chem. Geol. 246, 39-54.

Cline, J. S., Bodnar, R. J., 1991. Can economic porphyry copper mineralization be generated by a typical calc-alkaline melt? J. Geophys. Res. 96, 8113-8126.

Driesner, T., Heinrich, C. A., 2007. The system H_2O–NaCl. Part I: Correlation formulae for phase relations in temperature–pressure–composition space from 0 to 1000 °C, 0 to 5000 bar, and 0 to 1 X_{NaCl}. Geochim. Cosmochim. Acta 71, 4880-4901.

Giggenbach, W. F., 1992. Magma degassing and mineral deposition in hydrothermal system along convergent plate boundaries. Econ. Geol. 87, 1927-1944.

Guillong, M., Heinrich, C. A., 2007. Sensitivity enhancement in laser ablation ICP-MS using small amounts of hydrogen in the carrier gas. J. Anal. At. Spectrom. 22, 1488-1494.

Guillong, M., Latkoczy, C., Seo, J. H., Günther, D. & Heinrich, C. A., 2008. Determination of sulfur in fluid inclusions by laser ablation ICP-MS, J. Anal. At. Spectrom. 23, 1581-1589.

Günther, D., Audétat, A., Frischknecht, R., Heinrich, C. A., 1998. Quantitative analysis of major, minor and trace elements in fluid inclusions using Laser Ablation-Inductively Coupled Plasma-Mass Spectrometry (LA-ICP-MS). J. Anal. At. Spectrom. 13, 263-270.

Gustafson, L. B., Hunt, J. P., 1975. The porphyry copper deposit at El Salvador, Chile, Econ. Geol. 70, 857-912.

Halter, W. E., Pettke, T., Heinrich, C. A., 2002. The origin of Cu/Au ratios in porphyry-type ore deposits. Science 296, 1844-1846.

Hattori, K., 1993. High-sulfur magma, a product of fluid discharge from underlying mafic magma: evidence from Mount Pinatubo, Philippines. Geology 21, 1083-1086.

Hedenquist, J. W., Simmons, S. F., Giggenbach, W. F., Eldridge, C. S., 1993. White Island, New Zealand, volcanic-hydrothermal system represents the geochemical environment of high-sulfidation Cu and Au ore deposition. Geology 21, 731-734.

Heinrich, C. A., Günther, D., Audétat, A., Ulrich, T., Frischknecht, R., 1999. Metal fractionation between magmatic brine and vapor, determined by microanalysis of fluid inclusions. Geology 27, 755-758.

Heinrich, C.A., Pettke, T., Halter, W.E., Aigner-Torres, M., Audétat, A., Günther, D., Hattendorf, B., Bleiner, D., Guillong, M., Horn, I., 2003. Quantitative multi-element analysis of minerals, fluid and melt inclusions by laser-ablation inductively-coupled plasma mass-spectrometry. Geochim. Cosmochim. Acta 67, 3473-3497.

Heinrich, C. A., Driesner, T., Stefánsson, A., Seward, T. M., 2004. Magmatic vapor contraction and the transport of gold from the porphyry environment to epithermal ore deposits. Geology 32, 761-764.

Heinrich, C. A., 2006. From fluid inclusion microanalysis to large-scale hydrothermal mass transfer in the Earth's interior. J. Min. Petrol. Sci. 101, 110-117.

Henley, R. W., McNabb, A., 1978. Magmatic vapor plumes and ground-water interaction in porphyry copper emplacement. Econ. Geol. 73, 1-20.

Klemm, L. M., Pettke, T., Heinrich, C. A., Campos, E., 2007. Hydrothermal evolution of the El Teniente deposit, Chile: Porphyry Cu-Mo ore deposition from low-salinity magmatic fluids, Econ. Geol. 102, 1021-1045.

Lehmann, B., 1990. Metallogeny of tin, in: Battacharji, S. et al. (Eds.) Lecture notes in earth sciences. Springer.

Lowenstern, J. B., Mahood, G. A., Rivers, M. L., Sutton, S. R., 1991. Evidence for extreme partitioning of copper into a magmatic vapor phase. Science 252, 1405-1409.

Mavrogenes, J. A., Bodnar, R. J., 1994. Hydrogen movement into and out of fluid inclusions in quartz: experimental evidence and geologic implications. Geochim. Cosmochim. Acta 58, 141-148.

Mavrogenes, J. A., Berry, A. J., Newville, M., Sutton, S. R., 2002. Copper speciation in vapor-phase fluid inclusions from the Mole Granite, Australia. Am. Mineral. 87, 1360-1364.

Mountain, B. W., Seward, T. M., 2003. Hydrosulfide complexes of copper (I): Experimental confirmation of the stoichiometry and stability of $Cu(HS)_2^-$ to elevated temperatures. Geochim. Cosmochim. Acta 67, 3005-3014.

Nagaseki, H., Hayashi, K., 2008. Experimental study of the behavior of copper and zinc in a boiling hydrothermal system. Geology 36, 27-30.

Palmer, D. A., Simonson, J. M., Jensen, J. P., 2004. Partitioning of electrolytes to steam and their solubilities in steam, in: Palmer, D. A., Fernández-Prini, R., Harvey, A. H. (Eds.), Aqueous systems at elevated temperatures and pressures: Physical chemistry in water, steam and hydrothermal solutions. Elsevier, pp. 407-439.

Pokrovski, G. S., Borisova, A. Y. & Harrichoury, J. C., 2008. The effect of sulfur on vapor-liquid fractionation of metals in hydrothermal systems. Earth Planet. Sci. Lett. 266, 345-362.

Ronacher, E., Richards, J. P., Reed, M. H., Bray, C. J., Spooner, E. T. C., Adams, P. D., 2004. Characteristics and evolution of the hydrothermal fluid in the north zone high-grade area, Porgera Gold Deposit, Papua New Guinea. Econ. Geol. 99, 843-867.

Rusk, B. G., Reed, M. H., Dilles, J. H., Klemm, L. M., Heinrich, C. A., 2004. Compositions of magmatic hydrothermal fluids determined by LA-ICP-MS of fluid inclusions from the porphyry copper-molybdenum deposit at Butte, MT. Chem. Geol. 210, 173-199.

Seward, T. M., 1984. The formation of lead (II) chloride complexes to 300°C: A spectrophotometric study. Geochim. Cosmochim. Acta 48, 121-134.

Seward, T. M., Barnes, H. L., 1997. Metal transport by hydrothermal ore fluids, in: Barnes, H. L. (Ed.), Geochemistry of Hydrothermal Ore deposits, third ed. Wiley, pp. 435-486.

Simon, A. C., Pettke, T., Candela, P. A., Piccoli, P. M., Heinrich, C. A., 2004. Magnetite solubility and iron transport in magmatic-hydrothermal environments. Geochim. Cosmochim. Acta 68, 4905-4914.

Simon, A. C., Pettke, T., Candela, P. A., Piccoli, P. M., Heinrich, C. A., 2006. Copper partitioning in a melt-vapor-brine-magnetite-pyrrhotite assemblage. Geochim. Cosmochim. Acta 70, 5583-5600.

Stefánsson, A., Seward, T. M., 2004. Gold (I) complexing in aqueous sulfide solutions to 500°C at 500 bar. Geochim. Cosmochim. Acta 68, 4121-4143.

Stoffell, B., Appold, M. S., Wilkinson, J. J., McClean, N. A., Jeffries, T. E., 2008. Geolchemistry and evolution of Mississippi Valley-Type mineralizing brines from Tri-State

and Northern Arkansas districts determined by LA-ICP-MS microanalysis of fluid inclusions. Econ. Geol. 103, 1411-1435.

Ulrich, T., Günther, D., Heinrich, C. A., 1999. Gold concentrations of magmatic brines and the metal budget of porphyry copper deposits. Nature 399, 676-679.

Webster, J. D., Mandeville, C. W., 2007. Fluid immiscibility in volcanic environments, in: Liebscher, A., Heinrich, C. A. (Eds.), Fluid-Fluid Interactions. Reviews in Mineralogy and Geochemistry, vol. 65. pp. 313-362.

Williams-Jones, A. E., Migdisov, A. A., Archibald, S. M., Xiao, Z., 2002. Vapor transport of ore metals, in: Hellmann, R., Wood, S. A. (Eds.), Water-Rock Interactions, Ore Deposits, and Environmental Geochemistry: a tribute to David A. Crerar, vol. 7. The Geochemical Society, pp. 279-305.

Williams-Jones, A. E., Heinrich, C. A., 2005. Vapor transport of metals and the formation of magmatic-hydrothermal ore deposits. Econ. Geol. 100th Anniv. vol., 1287-1312.